

Absolute and Relative Nonlinear Optical Coefficients of KDP, KD*P, BaB₂O₄, LiIO₃, MgO:LiNbO₃, and KTP Measured by Phase-Matched Second-Harmonic Generation

ROBERT C. ECKARDT, MEMBER, IEEE, HISASHI MASUDA, YUAN XUAN FAN, AND ROBERT L. BYER, FELLOW, IEEE

Abstract—Both absolute and relative measurements of the nonlinear optical coefficients of six nonlinear materials were measured by second-harmonic generation. A single-mode, injection-seeded, *Q*-switched Nd:YAG laser with spatially filtered output was used to generate the 1.064 μ m fundamental radiation. The following results were obtained: d_{36} (KDP) = 0.38 pm/V, d_{36} (KD*P) = 0.37 pm/V, $|d_{22}(\text{BaB}_2\text{O}_4)|$ = 2.2 pm/V, $d_{31}(\text{LiIO}_3)$ = -4.1 pm/V, $d_{31}(5\% \text{MgO:LiNbO}_3)$ = -4.7 pm/V, and d_{eff} (KTP) = 3.2 pm/V. The accuracy of these measurements is estimated to be better than 10%.

I. INTRODUCTION

CAREFUL measurements of the nonlinear optical coefficients of several nonlinear crystals of current technical interest are presented. These measurements were made by phase-matched second-harmonic generation using a *Q*-switched Nd:YAG laser operating at 1.064 μ m as the source of fundamental radiation. The laser was injection seeded to operate in a single longitudinal mode, and the output was spatially filtered to produce a Gaussian-like transverse distribution. Characterization of the pump pulse and calibration of the apparatus indicated that these measurements should be accurate to better than 10%.

This measurement was originally intended to be only a determination of the nonlinear coefficient of barium metaborate (BaB₂O₄), an interest that was motivated by observations of optical parametric oscillator thresholds that were below expected values [1]. The measurement grew to include several other nonlinear optical materials that are commonly used for second-harmonic generation pumped by 1.06 μ m radiation. The additional materials

Manuscript received November 29, 1989. This work was supported by the U.S. Army Research Office under Contract DAAL03-88-K-0113 and by NASA under Grant NAGW 1760.

R. C. Eckardt and R. L. Byer are with the Ginzton Laboratory, Stanford University, Stanford CA 94305.

H. Masuda was on leave at the Ginzton Laboratory, Stanford University, Stanford CA 94305. He is with the Corporate Research Laboratories, Sony Corporation, 1-7-4, Kohnan, Minato-ku, Tokyo 108, Japan.

Y. X. Fan is with LaserGenics, Inc., San Jose, CA 95131.

IEEE Log Number 9034738.

were measured because of a current controversy concerning the absolute magnitude of nonlinear coefficients.

Our observations use both absolute and relative measurements of nonlinear coefficients. The absolute measurements yielded values consistent with other second-harmonic measurements. Measurements performed with high-power well-characterized lasers and potassium dihydrogen phosphate [2] have yielded the value d_{36} (KDP) = 0.39 pm/V, which has become accepted in the application of high-power harmonic conversion for fusion research [3]. Earlier CW measurements of 633 to 316 nm harmonic generation in ammonium dihydrogen phosphate gave a value of d_{36} (ADP) = 0.57 pm/V [4], [5]. Combining this with relative measurements between KDP and ADP yields d_{36} (KDP) = 0.41 pm/V [6]. We measured d_{36} (KDP) = 0.38 pm/V, in good agreement with both earlier harmonic measurements. Values for d_{36} (KDP) determined by the technique of parametric fluorescence [7], [8] tend to be higher. Previously, the value for 1.06 μ m-532 nm harmonic generation in lithium iodate $d_{31}(\text{LiIO}_3)$ = -7.1 pm/V based on parametric fluorescence had been accepted as standard [9]. (No attempt was made to measure signs of the nonlinear coefficients; however, when the signs are known [6], they are included.) On the parametric fluorescence LiIO₃ scale, the coefficient for potassium dihydrogen phosphate is d_{36} (KDP) = 0.63 pm/V for second-harmonic generation pumped by 1.06 μ m radiation [7]. Clearly, there is a discrepancy in the accepted values for nonlinear optical coefficients.

The crystals included in the measurements reported here are KDP, LiIO₃, BaB₂O₄, potassium dideuterium phosphate (KD*P), potassium titanyl phosphate (KTP), and magnesium oxide-doped lithium niobate (5% MgO:LiNbO₃). The ratio of d_{36} (KDP) to $d_{31}(\text{LiIO}_3)$ obtained in these measurements is in agreement with earlier measurements [7]. However, the value of $d_{31}(\text{LiIO}_3)$ is only 58% of the parametric fluorescence value presented in [9]. The reason for the variance is not understood. It has been suggested that the pump wavelengths may have been too close to the LiIO₃ absorption edge in the parametric fluorescence measurements. There has also

been some question of the necessity for further corrections to deal with the birefringence of the nonlinear crystals. An anisotropic Green's function analysis [10] is discussed in the Appendix, with the conclusion that existing theory is appropriate for the quantitative analysis of near-field second-harmonic generation and parametric fluorescence.

The advantage of parametric fluorescence is that it is only necessary to measure the power ratio of the pump radiation and the generated fluorescence, whereas second harmonic requires the measurement of an absolute power and the spatial and temporal distributions of the pump field. Phase matching is also of critical importance in the second-harmonic technique. Second-harmonic generation, however, has the advantage that it is a direct measurement of the nonlinear coefficient under conditions that more closely duplicate actual applications. The results presented here are a study of nonlinear coefficient measurement by second-harmonic generation. At this point, no attempt is made to explain the different values obtained by the two techniques. In the future, more work is needed to resolve these apparent differences.

Our second-harmonic measurements were performed under near-field conditions where diffraction is not of concern. Birefringent walkoff, however, was significant in the longer angle-tuned crystals. A Gaussian transverse intensity distribution was assumed, and the focused beam analysis of Boyd and Kleinman [11] was used. This CW analysis was extended to pulsed harmonic generation by numerical integration of the observed temporal distribution. Substantial effort was placed in characterizing the temporal and spatial distribution of the pump pulse. The largest single source of error in these measurements is fluctuation in spatial distribution caused by drifting of spatial filter alignment. This single error source is about equal in magnitude to all other sources of error combined.

The highest levels of harmonic conversion used here were 14%, a level at which pump depletion must be considered, but can be treated adequately with a simple near-field approximation. The depletion approximation was verified by observation of the dependence of harmonic conversion on pump energy in two crystals. Measurements to demonstrate that two-photon absorption was not a factor were also performed in the same crystals. In all cases, phase-matching tuning curves were carefully compared to calculated curves obtained from dispersion relations. The agreement of observed and theoretical tuning curves assured that the full length of the nonlinear crystal was used, and that optical distortions were not limiting harmonic conversion.

The theoretical development used to analyze our second-harmonic measurements is discussed in Section II. Although no new theory is presented, except for the depletion approximation, the theory is presented to make explicit the definitions that are used to describe the second-harmonic generation interaction. Different factors appear in the various methods of presentation, and misinterpretation of factors abound in this field. The

experimental apparatus is described in Section III, and measurements are discussed in Section IV. Results are summarized in Section V.

II. THEORY

The analysis used here draws almost entirely from earlier work [11], [12] which is reviewed in many places [6], [9], [13], [14]. MKS units are used. Definition of notation is made using a few expressions appropriate for monochromatic planewaves. The discussion continues by including the focused beam analysis, and is extended to pulsed harmonic conversion by numerical integration using observed pulse shapes. A simple approximation derived empirically by calculation is used to allow for the small amount of fundamental wave depletion in the measurements. Finally, a near-field approximation is used to allow for an elliptical transverse beam distribution.

The electric field or electric polarization, both of which are real, can be expressed as the product of a complex amplitude and exponential summed with the complex conjugate of that product. In this format, the time-dependent electric field of a monochromatic plane wave of angular frequency ω is

$$E(\mathbf{r}, t) = \frac{1}{2} E(\mathbf{r}, \omega) \exp \{i(\mathbf{k} \cdot \mathbf{r} - \omega t)\} + \text{c.c.}$$

The relationship between the vector components of electric polarization at the harmonic frequency 2ω resulting from the second-order nonlinear interaction define the nonlinear optical coefficients $d_{jkl}(-2\omega, \omega, \omega)$:

$$\mathcal{P}_i^{NL}(\mathbf{r}, 2\omega) = \sum_{j,k=1}^3 \epsilon_0 d_{ijk}(-2\omega, \omega, \omega) E_j(\mathbf{r}, \omega) E_k(\mathbf{r}, \omega) \quad (1)$$

where ϵ_0 is the permittivity of free space. The reduced notation $d_{ijk} \rightarrow d_{im}$ allows the representation of the nonlinear optical coefficients in the customary 3×6 matrix. Further reduction to a single effective nonlinear coefficient d_{eff} dependent on nonlinear optical properties, phase matching, and crystal orientation is standard for modeling phase-matched second-harmonic generation. With this notation, the coupled equations describing harmonic generation for a monochromatic plane wave propagating in the z direction are

$$\frac{d}{dz} E(z, 2\omega) = i\kappa e^{-i\Delta kz} E^2(z, \omega) \quad (2a)$$

and

$$\frac{d}{dz} E(z, \omega) = i\kappa e^{i\Delta kz} E(z, 2\omega) E^*(z, \omega) \quad (2b)$$

where $\kappa = \omega d_{\text{eff}} / (nc)$ with n the index of refraction, c the speed of light, and $\Delta k = k_{2\omega} - 2k_\omega$ the wave vector mismatch. Two elementary solutions to the coupled equations are

$$I_{2\omega}(l) = I_\omega(0) \left\{ \Gamma l \sin(\Delta kl/2) / (\Delta kl/2) \right\}^2 \quad (3a)$$

and

$$I_{2\omega}(l) = I_\omega(0) \tanh^2(\Gamma l) \quad (3b)$$

for the respective cases of negligible pump depletion and perfect phase matching. Here, $I_{2\omega}(l)$ is the harmonic intensity generated in a crystal of length l , $I_\omega(0)$ is the initial fundamental intensity, and $\Gamma^2 = 2\kappa^2 I_\omega(0)/(cn\epsilon_0)$. Any of (1), (2), or (3) can serve to define the notation used to express the nonlinear coefficients.

The dispersion in the nonlinear coefficient $d_{jkl}(-2\omega, \omega, \omega)$ is often expressed in using Miller's delta [15] δ_{jkl} and the linear susceptibilities

$$\begin{aligned} d_{ijk}(-2\omega, \omega, \omega) &= \epsilon_0 \chi_{ii}^{2\omega} \chi_{jj}^{\omega} \chi_{kk}^{\omega} \delta_{ijk} \\ &= \epsilon_0 \{n_i^2(2\omega) - 1\} \{n_j^2(\omega) - 1\} \\ &\quad \cdot \{n_k^2(\omega) - 1\} \delta_{ijk}. \end{aligned} \quad (4)$$

Here, $\chi_{ii}^{2\omega}$ is the linear electric susceptibility at frequency 2ω , and $n_i(2\omega)$ is the index of refraction at 2ω , both for light with the electric field polarized in the direction of the i th principal axis of the crystal. The dispersion of δ_{jkl} has been demonstrated to be small, and for experimental purposes, δ_{jkl} is usually treated as a constant.

Beam characterization measurements described in the next section show that the transverse distribution of our beam is nearly Gaussian in shape. Second-harmonic conversion efficiency for CW beams with Gaussian transverse distribution in the low conversion limit is given by [11], [13]

$$\eta_{\text{CW}} = p_{2\omega}/p_\omega = 2\omega^2 d_{\text{eff}}^2 p_\omega lkh(B, \xi)/(\pi n^3 \epsilon_0 c^3) \quad (5)$$

where p_ω and $p_{2\omega}$ are the powers of incident fundamental (after surface losses) and the output second harmonic (before surface losses), respectively. The Boyd and Kleinman focusing factor $h(B, \xi)$ is a function of the walkoff parameter B and focusing parameter ξ , which are expressed by the formulas

$$B = \rho \sqrt{lk}/2 \quad (6)$$

and

$$\xi = l/(kw_0^2). \quad (7)$$

Here, ρ is the birefringent walkoff angle, w_0 is the $1/e$ amplitude radius at the beam waist, and $k = nw/c$ is the magnitude of the fundamental wave vector inside the crystal.

For beam parameters used in these measurements, the approximations of $h(B, \xi)$ for the limiting case of weak focusing $\xi \ll 1$ are appropriate. With the added constraints of optimum phase matching, no absorption, and birefringent walkoff aperture length greater than crystal length $l_a = \pi^{1/2} w_0/\rho > l$, the focusing factor is given to the necessary accuracy by

$$h(B, \xi) \approx \xi(1 - t^2/12 + t^4/120 - t^6/1344 + \dots) \quad (8)$$

where $t = 2B(2\xi)^{1/2}$. Since (8) assumes perfect phase matching, numerical solutions of the double integral defining $h(B, \xi)$ [11] were used to calculate phase-matching curves for angle-tuned crystals. Equation (8) does not in-

clude bulk material losses; however, using (8) and approximating bulk losses as surface losses gave the required accuracy for a 1 cm KDP crystal. None of the other crystals used had significant absorption.

The extension of (5) to pulsed harmonic conversion was accomplished with an integration over the observed pulse shape; $u = \int p(t) dt = P\Delta t$ where u is the total energy, $p(t)$ is the instantaneous power, P is the peak power, and Δt is an effective pulse width. Here, Δt_ω and $\Delta t_{2\omega}$ were obtained by numerical integration of the observed fundamental pulse shape and the square of the observed fundamental pulse shape, respectively. This treatment is applicable when the pulse has no structure or modulation on the scale picoseconds or shorter, which would make group velocity walkoff important. Rewriting (5) for pulsed harmonic conversion,

$$\begin{aligned} \eta_{\text{calc}} &= \frac{u_{2\omega}}{u_\omega} = \frac{P_{2\omega} \Delta t_{2\omega}}{P_\omega \Delta t_\omega} \\ &= 2u_\omega \omega^2 d_{\text{eff}}^2 \frac{\Delta t_{2\omega}}{\Delta t_\omega^2} \frac{lkh(B, \xi)}{\pi n^3 \epsilon_0 c^3}. \end{aligned} \quad (9)$$

The subscript is used to indicate that η_{calc} is the conversion efficiency that is obtained from a calculation that assumes no pump depletion. Pump depletion was approximated with the relation

$$\eta_{\text{calc}} = \eta_{\text{observed}} / (1 - \eta_{\text{observed}}) \quad (10)$$

where η_{observed} is the observed energy conversion efficiency. Numerical integration for the near field without walkoff showed that (10) is accurate to better than 2% for $\eta_{\text{observed}} < 50\%$.

Allowance was also made for an elliptical transverse distribution of the pump beam, a condition that existed in some of these measurements. A pump traveling in the z direction with intensity distribution which is described by

$$I_\omega = I_0 \exp(-2x^2/w_x^2 - 2y^2/w_y^2)$$

is used. For the near-field approximation, it is necessary to retain the walkoff dependence of the focusing parameter in the critical phase-matching direction which is chosen to be the x direction. However, the beam area must be adjusted to allow for a different size in the noncritical y direction. This is done with the substitution

$$h(B, \xi) \rightarrow (w_x/w_y)h(B, \xi_x); \quad \xi_x = l/(kw_x^2). \quad (11)$$

When the pump depletion approximation and the allowance for elliptical transverse distribution are included, (9) solved for d_{eff}^2 becomes

$$d_{\text{eff}}^2 = \frac{(u_{2\omega}/u_\omega^2)}{(1 - u_{2\omega}/u_\omega)} \frac{\Delta t_\omega^2}{\Delta t_{2\omega}} \frac{w_y}{w_x} \frac{c\epsilon_0 n^2 \lambda_0^3}{16\pi^2 l h(B, \xi_x)}. \quad (12)$$

In (12), both $\omega = 2\pi c/\lambda_0$ and $k = 2\pi n/\lambda_0$ have been expressed in terms of the free-space wavelength λ_0 of the fundamental radiation.

The expressions for the effective nonlinear coefficients of the materials used are reproduced in Table I. The effect of nonorthogonality of the extraordinary electric field with the wave vector in the birefringent crystals is included.

TABLE I
EFFECTIVE NONLINEAR OPTICAL COEFFICIENTS

Crystal	Point Group	Phase-Matching	Effective Nonlinear Optical Coefficient ^a
KDP	$\bar{4}2\text{ m}$	Type I	$d_{\text{eff}} = -d_{36} \sin(\theta + \rho) \sin 2\phi$
KD*P		Type II	$d_{\text{eff}} = (d_{14} + d_{36}) \sin(\theta + \rho) \cos(\theta + \rho) \cos 2\phi$
BaB ₂ O ₄	3 m	Type I	$d_{\text{eff}} = d_{31} \sin(\theta + \rho) - d_{22} \cos(\theta + \rho) \sin 3\phi$
5% MgO:LiNbO ₃			
LiIO ₃	6	Type I	$d_{\text{eff}} = d_{31} \sin(\theta + \rho)$
KTP ^b	mm^2	Type II	$d_{\text{eff}} \approx (d_{24} - d_{15}) \sin 2\theta \sin 2\phi - (d_{15} \sin^2 \phi + d_{24} \cos^2 \phi) \sin \theta$

^aThere are different conventions used for defining effective nonlinear coefficients. We choose the one in which the direction of the wave vector is specified by spherical coordinates (θ, ϕ) referenced to the crystalline axes; ρ is the birefringent walkoff angle. The positive sense of the extraordinary polarization is taken as that which has a component in the direction of the positive crystalline z axis.

^bThe expression for KTP is an approximation that is justified by the small difference between n_x and n_y compared to the difference between n_x and n_z or n_y , and further justified because $\theta \approx 90^\circ$ for all measurements used here.

TABLE II
CALCULATED PHASE-MATCHING PARAMETERS

Crystal	Reference ^a	θ_{pm}	ρ	$n_0(\omega)$	$n_e(\omega)$	$n_0(2\omega)$	$n_e(2\omega)$
KDP, Type I	[17]	41.2°	1.60°	1.4942	1.4603	1.5129	1.4709
KD*P, Type I	[18]	36.6°	1.45°	1.4931	1.4582	1.5073	1.4683
KD*P, Type II		53.7°	1.42°, 1.28°				
BaB ₂ O ₄ , Type I	[19]	22.8°	3.19°	1.6545	1.5392	1.6742	1.5547
LiIO ₃ , Type I	[20]	30.2°	4.26°	1.8559	1.7164	1.8975	1.7475
5% MgO:LiNbO ₃ ^b , Type I	[21]	90°	0	2.2327	2.1527	2.3242	2.2327
$T = 107\text{ C}$							
KTP ^c , Type II	[22]	$\theta = 90^\circ$		$n_x(\omega) = 1.7381$		$n_x(2\omega) = 1.7785$	
		$\phi = 24.3^\circ$	0.19°	$n_y(\omega) = 1.7458$		$n_y(2\omega) = 1.7892$	
			0.26°	$n_z(\omega) = 1.8302$		$n_z(2\omega) = 1.8894$	

^aReference is to source of dispersion equations from which parameters are calculated.

^bLiNbO₃ is the only temperature tuned crystal; all the others are angle tuned at room temperature.

^cKTP is a biaxial crystal; all the others are uniaxial.

For negative uniaxial crystals, this is done by replacing θ with $\theta + \rho$ [11] in expressions such as those given by Midwinter and Warner [16]. Here, θ is the phase-matching angle and ρ is the birefringent walkoff angle. For LiIO₃, which has a relatively large walkoff angle, the magnitude of the value of d_{36} obtained from a measured value of d_{eff} is reduced. Indexes of refraction and phase-matching parameters calculated from dispersion equations are given in Table II.

III. EXPERIMENT SETUP

Measurements were performed in sets that involved the comparison of two nonlinear crystals. One crystal was a well-characterized reference, and the other was the crystal under test. Each set included absolute measurement of the individual crystals and a relative measurement. Phase-matching tuning curves were observed for both crystals, and surface reflections and total transmissions were measured at both fundamental and harmonic frequencies. Transverse beam characterizations were performed in the course of a measurement set, and the temporal pulse shape was monitored throughout the measurements. Other calibrations and consistency checks were performed on a less regular basis.

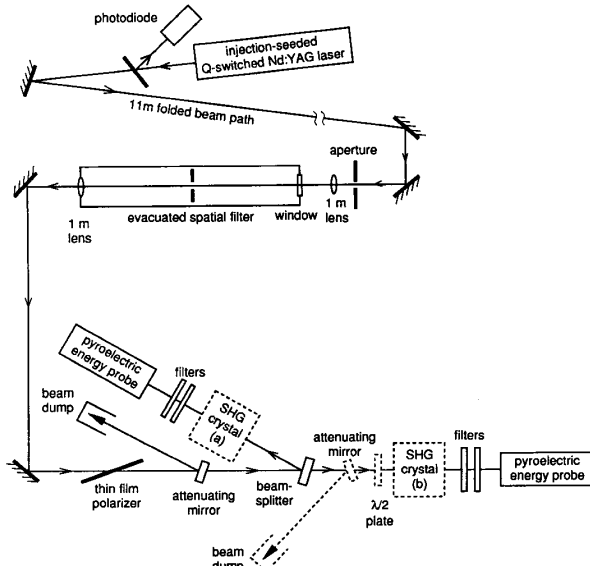


Fig. 1. Schematic drawing of experimental setup.

Fig. 1 shows the main components of the experimental setup which consisted of a *Q*-switched Nd:YAG laser, a spatial filter, and a two-beam arrangement in which the

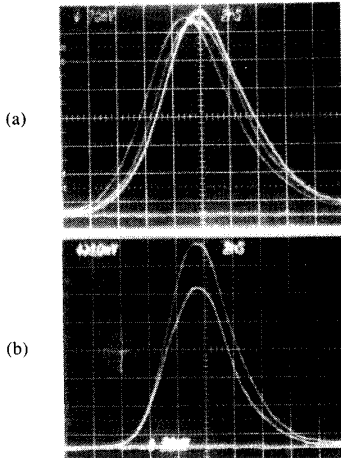


Fig. 2. Oscillograms showing fundamental (a) and second-harmonic (b) pulses. The time scale for both is 2 ns/cm displayed on the horizontal axis. Vertical displacement is relative power.

nonlinear crystals were measured and compared. An important feature of these measurements was the use of a single-mode injection-seeded laser for the 1.064 μm pump source. Temporal properties of the laser output were determined with a 0.4 ns rise time photodiode-oscilloscope combination and a Fabry-Perot interferometer with 0.03 cm^{-1} resolution. The measurements showed that the injection-seeded laser operated in a single axial mode. We expect that the spectral distribution was near the time-bandwidth limit for the 7.0 ± 0.2 ns full width at half maximum pulse.

Pulse duration changed little over the course of these measurements. Typical oscillograms of both fundamental and harmonic pulses are shown in Fig. 2. The leading and trailing edges of the fundamental pulse had exponential shapes, with a 1.4 ns time constant for the rise and 3.0 ns for the fall. Numerical integration over the measured pulse shape yielded the effective pulse width $\Delta t_\omega = 8.1 \pm 0.2$ ns and the ratio $\Delta t_{2\omega}/\Delta t_\omega = 0.67 \pm 0.02$. The ratio $\Delta t_{2\omega}/(\Delta t_\omega)^2 = 8.3 \times 10^7 \text{ s}^{-1} \pm 3\%$ was used in evaluating (12). The time response and time base calibration of the photodiode-oscilloscope combination were checked by observing the output of a mode-locked Nd: YAG laser. The time base was accurate to within 0.6%.

Shot-to-shot energy fluctuations were caused by drifting in the alignment of the spatial filter. Fig. 3(a) shows a histogram of individual pulse energy distribution. Most of the harmonic generation measurements consisted of averages obtained with 100 pulses. Several such averages were used in a measurement. Using 100-shot averages simplified the problem of shot-to-shot energy fluctuations and was consistent with the knife-edge transverse beam characterizations which were done with several hundred pulses. The histogram of pulse energies shows reasonable agreement with a normal distribution for which the probability of finding the fundamental energy between u_ω and $u_\omega + du_\omega$ is given by $P(u_\omega) du_\omega$ where

$$P(u_\omega) = \exp \left\{ - (u_\omega - \bar{u}_\omega)^2 / (2\sigma_\omega^2) \right\} / (\sigma_\omega \sqrt{2\pi}). \quad (13)$$

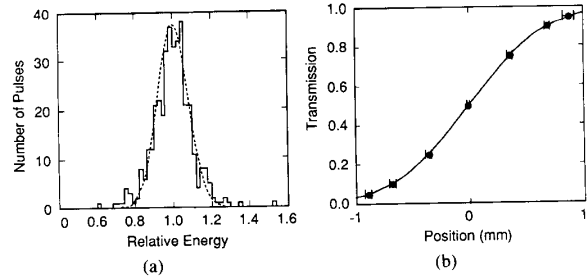


Fig. 3. Measurements characterizing laser output. (a) Histogram showing fundamental pulse energy distribution. (b) Typical knife-edge measurement of transverse beam distribution and calculated transmission for a Gaussian distribution fit to the data points. Error bars were obtained using eight separate horizontal and vertical scans performed over the course of one day.

\bar{u}_ω is the average fundamental energy, and σ_ω is the standard deviation. We observed $\sigma_\omega/\bar{u}_\omega = 0.08$. The standard deviation for harmonic pulses was 16%. However, the 100-shot averages reduced this value by a factor of ten. Averaging the shot-to-shot fluctuations will slightly bias harmonic measurements to higher values of harmonic power, as is seen by calculating the average value of u_ω^2 given by (13):

$$\langle u_\omega^2 \rangle = (\bar{u}_\omega)^2 + \sigma_\omega^2.$$

The bias was only 0.6% and was not included in the calculation.

Spatial filtering was performed by a combination of propagation into the far field, followed by aperturing the central peak of the distribution, and finally focusing through a pinhole in a vacuum spatial filter followed by recollimation. The output beam was slightly converging and reached a beam waist about 2 m beyond the collimating lens. Beam radii were measured by a knife-edge method at several positions after the collimating lens. It was demonstrated that the beam propagation closely followed that predicted for a Gaussian distribution. Aperture and pinhole adjustment in the spatial filter provided beam waists between $w_0 = 0.9$ and 1.6 mm.

Additional checks demonstrated that there were no extraneous temporal or spectral components in the laser output. No change in beam size due to a possible second spectral component was observed with the knife-edge characterization when two prisms were used in place of turning mirrors to provide a dispersion of 4 nm/mm. Photodiodes with various integrating times and sensitivities were used with different triggering and sweep rate settings of the oscilloscope, and no observable temporal components other than the Q -switched pulse were found in the laser output.

Repeated measurements of beam distribution were performed at the position where the SHG crystals were placed. The two-beam arrangement allowed quick measurements of the 0.05, 0.1, 0.25, 0.5, 0.75, 0.9, and 0.95 transmission positions as the knife-edge was scanned across the beam in one channel. The seven measurements were averaged to locate the center of the beam, and each of the six measurements other than the 0.5 position yielded a measurement of w_x or w_y . If the horizontal and vertical

measurements agreed within experimental error, they were combined to a single value w_0 , and if not, the beam would be treated as elliptical in shape. Fig. 3(b) shows the beam transmittance for knife-edge positions compared to values calculated for a Gaussian distribution. Typical individual beam scans yielded $\pm 3\%$ standard deviation for waist measurements. Eight measurements made over the course of one day combined to yield a standard deviation of $\pm 5\%$, which was taken as the accuracy to which the beam waist was known.

The components of the two-beam arrangement were easily rearranged and interchanged for a variety of measurements. The pump beam was transmitted through a thin film polarizer and a partially transmitting mirror to provide 2–4 mJ of linearly polarized 1.064 μm radiation incident on the beamsplitter. Beamsplitting ratios from 50/50 to 93/7 were used. The pyroelectric energy probes used to measure pulse energy had flat spectral response and could monitor both fundamental and harmonic. Absorbing glass filters and highly reflecting dielectric mirrors were used to eliminate fundamental radiation and transmit harmonic radiation when necessary. Calibrated neutral density filters and diffusers were used to keep measured fundamental intensities within the range of the energy probes. In addition to absolute and relative harmonic generation measurements, the apparatus also was used to measure transmissions of crystals and filters. Surface reflectivities of the crystals at both fundamental and harmonic were measured with rearrangement of components, and transmission at 532 nm was measured with the harmonic output generated in a separate crystal.

Three axes of rotational adjustment were used in the crystal mounts. Two of the axes were perpendicular to the direction of polarization and a third was parallel. A polarized alignment beam was used to determine whether the crystals were properly oriented with respect to the pump beam. A half-wave plate was used to rotate the fundamental polarization for maximum harmonic generation for measurements with type II crystals. The angular adjustments allowed rotation through a small range of azimuthal angle to check that the crystals were properly oriented for maximum d_{eff} . All the crystals were properly oriented. However, it was necessary to use the 12 mm BaB₂O₄ crystal significantly off normal incidence to avoid problems of parallel-surface reflections.

The calibrations of the two pyroelectric energy probes were intercompared, and each pyroelectric probe was compared to a thermoelectric power meter. The power meter was internally calibrated with an electrical resistance heater. The 30 Hz repetition rate of the laser allowed comparison of the average power measurement with the average pulse energy of the pyroelectric probes. The thermoelectric power meter read 3% higher than the higher of the two pyroelectric energy probes, and that probe gave a reading 2% higher than the other; all agreed within 5%. The relative difference of the two probes was retained in the analysis of data, and their average reading was used as the energy calibration. The reason for this choice was that conditions were more appropriate for the pyroelectric detectors, and the 5% difference is within the

expected error of all the meters and is too small to be significant. The 5% value was taken as the accuracy of the energy measurement, which also is the accuracy stated by the manufacturer.

Energy measurement was also dependent on the accuracy of filter, attenuator, and beamsplitter calibration. Filters and attenuators were measured both in the two-beam setup described above and with a spectrophotometer. Comparison indicated accuracies of 1% in the measured transmissions. The beamsplitting ratio and probe sensitivity ratio were checked repeatedly to assure consistency in the measurements. Variations of 1/2–1% caused by differences in probe placement and pointing were found. Where possible, critical parameters were measured with more than one method, and multiple or additional measurements were used for consistency checks and determination of accuracy.

The overall accuracy of these nonlinear coefficient measurements is estimated to be better than 10%. The average of the harmonic energy divided by the square of the fundamental energy $\langle u_{2\omega}/u_\omega^2 \rangle$ was determined for each series of 100 shots in making absolute measurements. A further average was made of at least five and usually more such measurements of $\langle u_{2\omega}/u_\omega^2 \rangle$. Typically, the individual averages in one set of measurements would be consistent to $\pm 2\%$. Larger variations were observed with repeated measurements that would entail recalibration, use of different samples of the same material, or different beam parameters. For example, 12 measurements on three different samples of BaB₂O₄ had a $\pm 3.6\%$ standard deviation for the value of d_{eff} . Examination of (12), however, shows that d_{eff} can only be determined to the accuracy to which w_0 was known, and that was estimated to be 5%. The accuracy of quantities $\Delta t_{2\omega}/(\Delta t_\omega)^2$ and $u_{2\omega}/u_\omega^2$ could double the uncertainty of the values of d_{eff} .

IV. MEASUREMENTS

12 separate absolute measurements were made on three different BaB₂O₄ samples, more than used for the other materials. Also, the other materials were all measured relative to BaB₂O₄. This discussion starts with the barium metaborate measurements. The discussion is then expanded to include other materials, both by absolute and relative measurement of the nonlinear coefficients.

Two of the three BaB₂O₄ samples were grown at the Stanford Center for Materials Research, and the third was grown at the Fujian Institute of Research on the Structure of Matter in the People's Republic of China. The Stanford crystals were 4.1 and 11.9 mm long, and the Fujian crystal was 9.4 mm long. The tuning curves for the three BaB₂O₄ crystals agreed well with tuning curves obtained from dispersion equations and numerical evaluation of the double integral that defines the Boyd and Kleinman focusing factor $h(B, \xi)$. The calculated tuning curves were adjusted for pump depletion using (10). The observed and calculated curves for the 11.9 mm crystal are shown in Fig. 4(a) and (b).

The effective nonlinear coefficient obtained in these measurements was $d_{\text{eff}}(\text{BaB}_2\text{O}_4) = 1.94 \pm 0.07 \text{ pm/V}$. The sign of the d_{31} coefficient relative to that of d_{22} is

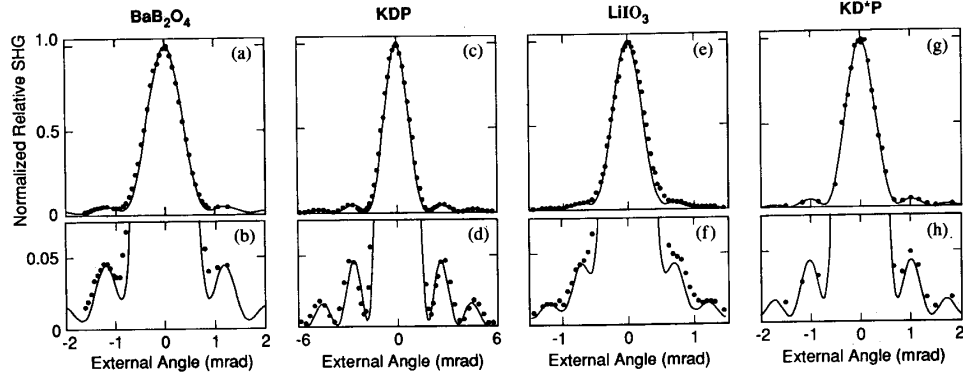


Fig. 4. Measured (data points) and calculated (solid lines) phase-matching tuning curves for different second-harmonic crystals.

unknown for BaB_2O_4 , and no effort was made to determine the polarity of the crystals that were measured. Fortunately, d_{31} is small compared to d_{22} ; measurements of $|d_{31}| = 0.07 |d_{22}|$ [23] and $|d_{31}| < 0.05 |d_{22}|$ [24] have been reported. Assuming that d_{31} is negligible, the value $|d_{22}| = 2.16 \pm 0.08 \text{ pm/V}$ is obtained from the measured d_{eff} , calculated phase-matching parameters (Table I) and the appropriate definition of d_{eff} (Table II). Expressing the result with two digits as $|d_{22}| = 2.2 \text{ pm/V}$ more correctly conveys the accuracy of the measurement.

Earlier measurements have placed $|d_{22}(\text{BaB}_2\text{O}_4)| = 4.1 d_{36}(\text{KDP})$ [23], [24]. The result of 2.2 pm/V is 37% higher than these earlier results when $d_{36}(\text{KDP}) = 0.39 \text{ pm/V}$ is used. Even though $|d_{22}(\text{BaB}_2\text{O}_4)| = 5.7 d_{36}(\text{KDP})$ was observed here, these measurements nearly duplicated the 0.39 pm/V result for KDP.

Only a single KDP crystal was measured. The 10.4 mm long crystal was oriented for type I phase matching, and surfaces were uncoated. The observed tuning curve again closely follows the calculated curve [Fig. 4(c) and (d)]. There is a smaller amount of birefringent walkoff in this crystal compared to the BaB_2O_4 crystal; therefore, the tuning curves more closely approach the sinc-squared curve of the monochromatic plane wave. Both absolute measurements of the KDP crystal and measurements relative to the 9.4 and 11.7 mm BaB_2O_4 crystals using $d_{\text{eff}}(\text{BaB}_2\text{O}_4) = (1.94 \pm 0.07) \text{ pm/V}$ were closely grouped at $d_{36}(\text{KDP}) = 0.376 \pm 0.005 \text{ pm/V}$. This small range of measurements could be coincidence, and the earlier comments about accuracy apply. More typically, the combined measurements on a single material would have $\pm 4\%$ standard deviation. For comparison, it is useful to mention that in the notation used by Craxton [2], $\{d_{36}(\text{KDP})/\epsilon_0\}_{\text{Craxton}} = 0.78 \text{ pm/V}$ corresponds to $d_{36}(\text{KDP}) = 0.39 \text{ pm/V}$ in the notation used here.

In contrast to the agreement with KDP second-harmonic measurements, these observations produced substantially different results compared to parametric fluorescence measurements of lithium iodate. Two LiIO_3 crystals, 14.7 and 19.8 mm long, were used for type I second-harmonic generation. These crystals were antireflection coated on input and output faces. Both crystals demonstrated good agreement between predicted and observed phase-matching curves. Birefringent walkoff was

again significant, as can be seen in the shape of the secondary maxima in the tuning curves of the 14.7 mm crystal. [Fig. 4(e) and (f)]. Absolute measurements of the two LiIO_3 crystals gave $|d_{31}| = 4.24 \pm 0.10 \text{ pm/V}$, whereas measurements relative to BaB_2O_4 and KDP, respectively, yielded 4.02 ± 0.19 and $4.08 \pm 0.19 \text{ pm/V}$. The value obtained by combining these measurements and using the known sign was $d_{31}(\text{LiIO}_3) = -4.1 \pm 0.2 \text{ pm/V}$.

Tabulations of measurements of the nonlinear coefficients of LiIO_3 [6] show an unusually wide range of values. Of concern was that the high intensities used for pulsed harmonic generation could lower efficiency through some third-order nonlinear effect such as two-photon absorption or intensity-dependent refractive indexes. Harmonic generation was observed as a function of fundamental pulse energy in an attempt to detect such effects. This was accomplished by attenuating the pump pulse with calibrated partially reflecting mirrors between the beam-splitter and the 19.8 mm LiIO_3 crystal. Fig. 5(a) shows the observed deviation from linearity between generated harmonic energy and square of the fundamental energy. This deviation was explained by pump pulse depletion as approximated by (10). There was no indication of reduced harmonic generation by any third-order process in this set of measurements. The four steps of attenuation gave five relative measurements of nonlinear coefficient at peak intensities ranging from 7.4 MW/cm^2 for the unattenuated pulse to approximately one-fifth that value. The five measurements had better consistency, $d_{31} = -4.13 \pm 0.05 \text{ pm/V}$, than other measurements made at constant intensity.

An additional measurement was performed to test for nonlinear absorption. Fundamental energy was monitored in the reference channel, and both transmitted fundamental and generated harmonic were measured in the test channel as the 19.8 mm LiIO_3 crystal was tuned through phase matching. The measurement of total transmission and observed and calculated tuning curves is shown in Fig. 6(a)-(c). The measurement suggested that two-photon absorption was present, but not large enough to significantly have changed the measurement of the nonlinear coefficient. The second surface of the crystal was antireflection coated for 532 nm, and a 0.5% increase in total transmission was expected at peak conversion, but not ob-

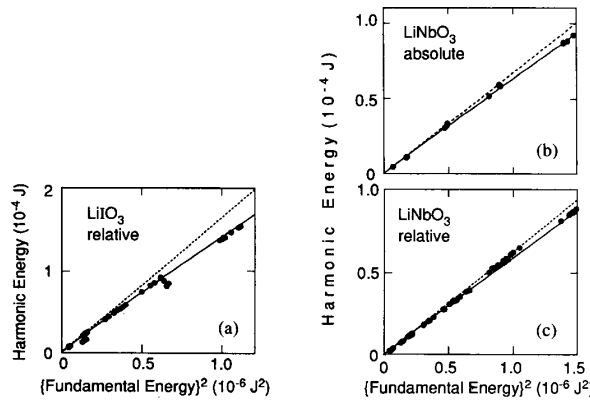


Fig. 5. Second-harmonic generation energy conversion as a function of incident fundamental energy squared for lithium iodate (a) and lithium niobate (b) and (c). Fundamental energy was measured directly in the absolute measurement and was deduced for the harmonic generation in a reference crystal for the relative measurements. The solid lines are the calculated conversion with pump depletion, and the dotted lines without. Each data point represents a 100-shot average. The LiIO₃ data points which fell obviously below the others were caused by unstable mounting of the crystal.

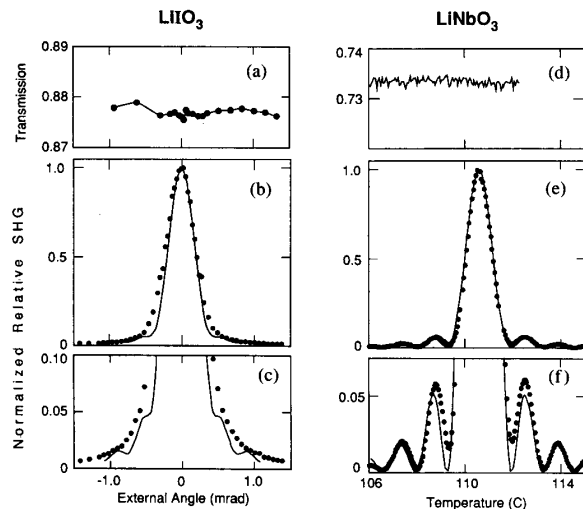


Fig. 6. Total transmission for combined fundamental and harmonic as LiIO₃ (a) and LiNbO₃ (d) crystals are tuning through phase matching. The line drawn in the transmission measurement simply connects the data points to make them more visible. The measured phase-matching tuning curves are shown by data points, and calculated tuning curves by the solid lines for LiIO₃ in (b) and (c) and for LiNbO₃ in (e) and (f).

served, suggesting that a few percent of the harmonic was lost by two-photon absorption.

Parametric fluorescence measurements have been previously performed for lithium niobate [25], [7], and it was of interest to compare second-harmonic generation measurements in this material. A 6.3 mm sample of 5% MgO:LiNbO₃ was prepared for temperature-tuned non-critically phase-matched second-harmonic measurements. This crystal was uncoated. The previous parametric fluorescence measurements were performed with stoichiometric and congruent LiNbO₃. The MgO:LiNbO₃ used

in these measurements has slightly different properties than those of stoichiometric or congruent compositions, but should be close enough for a useful comparison of the two techniques of nonlinear coefficient measurement. Congruent LiNbO₃ must be cooled below room temperature for noncritical-phase-matched second-harmonic generation pumped by 1064 nm radiation, but 5% MgO:LiNbO₃ has a phase-matching temperature near 107° C [26]. The MgO-doped material also has the advantage of reducing photorefractive damage [27], and is of interest for its application in external monolithic resonant cavity nonlinear frequency conversion [28].

The measurements performed on LiNbO₃ were similar to those described above for LiIO₃. There is no birefringent walkoff for 90° phase matching, and the tuning curve is expected to be the sinc-squared curve with the adjustment for pump depletion. The observed curve followed the calculated curve closely [Fig. 6(e) and (f)], except for a small deviation near the first minima. This was probably due to a distortion of the pump beam at the surface of the crystal. The excellent agreement in the locations of the secondary maxima and minima indicated that the full length of the crystal was used in the phase-matched interaction. The total transmission measurement of the crystal tuned through phase matching [Fig. 6(d)] shows no indication of two-photon absorption. The difference in second surface transmission for fundamental and harmonic was insignificant in the uncoated, phase-matched crystal.

Absolute measurements and measurements relative to BaB₂O₄ and KDP yielded an average value of d_{31} (5% MgO:LiNbO₃) = -4.69 ± 0.13 pm/V. With all the materials measured, both absolute and relative measurements had a reproducibility of 4%. This was further demonstrated by the measurements of pump-energy-dependent harmonic generation shown in Fig. 5(b) and (c). One measurement was absolute, with fundamental energy monitored in the reference channel. The other was a relative measurement where the second harmonic generated in a BaB₂O₄ crystal was monitored in the reference channel and fundamental energy was deduced from the reference harmonic signal. The two measurements give essentially the same result, with the depletion approximation again adequately describing the deviation from linearity in the ratio of harmonic energy to the square of the fundamental energy.

The measured coefficient d_{31} (5% MgO:LiNbO₃) = -4.7 pm/V is only 79% of the parametric fluorescence value for congruent LiNbO₃, not an unreasonable agreement considering that the materials have a different composition. This is supported by comparison measurements [29] of second-harmonic generation by 9 mm samples of MgO-doped and congruent materials under similar pumping conditions; 50.9% conversion was observed in the congruent material, and 35.2% conversion was observed in the MgO-doped material.

Two additional materials, KD*P and KTP, commonly used for 1064 nm pumped harmonic generation were studied. Two 30 mm long KD*P crystals, one each of type I and type II, were measured. For the type II crystal, the result of a quantitative analysis derived from a near-field

calculation was used, and Kleinman symmetry was used to set $d_{36} = d_{14}$. The KD*P crystals were measured both absolutely and relative to BaB_2O_4 , with the result $d_{36}(\text{KD*P}) = 0.367 \pm 0.012 \text{ pm/V}$. This is consistent with earlier measurements relative to KDP [30], [31], [32] which yielded values in the range $d_{36}(\text{KD*P}) = 0.34\text{--}0.48 \text{ pm/V}$ when normalized to $d_{36}(\text{KDP}) = 0.39 \text{ pm/V}$ [3] or $d_{36}(\text{KDP}) = 0.41 \text{ pm/V}$ [6]. The tuning curves for the two KD*P crystals both indicated high-quality material and little distortion of the pump beam. The tuning curve of the type I crystal is shown in Fig. 4(g) and (h).

Second-harmonic generation was observed in three type II KTP crystals. All the KTP crystals were produced by the flux growth technique in the People's Republic of China. The very parallel surfaces of the first two crystals produced interference which was seen in the tuning curve (Fig. 7). The third crystal was also very parallel, but had a 1064 nm antireflection on one surface and a 532 nm antireflection coating on the second surface. The observed tuning curve for this crystal was in excellent agreement for rotations both about the z axis and about an axis in the $x\text{-}y$ plane as shown in Fig. 8. This agreement indicates a crystal of excellent optical quality, with proper orientation, and very small distortion of the pump beam. The polarization of the fundamental pulse was rotated with a half-wave plate to produce the maximum second harmonic. The effective nonlinear optical coefficient derived from absolute harmonic measurements and measurements relative to KDP, KD*P, and BaB_2O_4 was $d_{\text{eff}}(\text{KTP}) = 3.18 \pm 0.17 \text{ pm/V}$. The value calculated from earlier measurements $|d_{24}| = 7.6 \times 10^{-12} \text{ m/V}$ and $|d_{15}| = 6.1 \text{ pm/V}$ [33] is $d_{\text{eff}}(\text{KTP})_{\text{calc}} = 7.3 \text{ pm/V}$ [22].

It is necessary to know the relative signs and relative magnitudes of d_{15} and d_{24} for the purpose of determining the size from a measurement of d_{eff} . Observation of the change in d_{eff} with crystal orientation indicates that d_{31} and d_{32} have the same sign. If it is assumed that the ratio $d_{24}/d_{15} = 1.25$ as measured previously [33], then the measured value of d_{eff} yields $|d_{24}| = 3.3 \text{ pm/V}$ and $|d_{15}| = 2.6 \text{ pm/V}$. These values are less than half of the earlier values. The measurements, complicated by interference, made with the uncoated KTP crystals ranged from $d_{\text{eff}} = 2.1$ to 4.4 pm/V and supported the measurement of the lower value.

V. SUMMARY

The nonlinear optical coefficient measurements reported here are summarized in Table III. These values can be taken as both relative measurements and absolute measurements. The reproducibility of the measurements was approximately $\pm 4\%$. When the values are used as relative measurements, the accuracy is the same as the reproducibility. It is possible that the absolute measurements could be biased by inaccuracy in modeling and fluctuations of the transverse beam distribution, measurement of pulse shape and duration, and by the accuracy of the energy measurements. It is estimated that the accuracy of

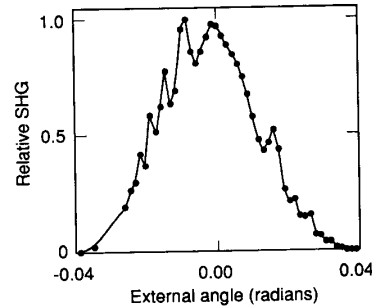


Fig. 7. A phase-matching tuning curve for an uncoated KTP crystal which has a problem of interference of reflections from the parallel surfaces.

the absolute measurements of the nonlinear coefficients is $\pm 10\%$.

The measurement for KDP reported here is in agreement with the nonlinear coefficient accepted for that material in high-power nonlinear conversion applications, and it agrees with the combination of relative measurements between KDP and ADP and low-power CW second-harmonic measurements with ADP. Furthermore, the relative measurements between KD*P and KDP and between KDP and LiIO_3 are in agreement with earlier measurements. There is possible agreement between the absolute measurement of 5% $\text{MgO} : \text{LiNbO}_3$ and parametric fluorescence measurements of congruent LiNbO_3 , but this is not conclusive. We have measured a significantly lower value for the nonlinear coefficients of KTP and a moderately higher value for the nonlinear coefficient of BaB_2O_4 than reported in earlier measurements. Perhaps the most significant difference is the absolute measurement of the nonlinear coefficient of LiIO_3 , which is only 58% of the value measured by parametric fluorescence.

It is remarkable that after more than 25 years of study in nonlinear optics, there should still exist such uncertainty in the scale of the nonlinear material parameters. This investigation indicates a need for further study. Performing both second-harmonic and parametric fluorescence measurements on the same nonlinear crystal samples would provide useful information. Such measurements would help resolve the difference in values observed for congruent LiNbO_3 and $\text{MgO} : \text{LiNbO}_3$. The anomaly between second-harmonic generation measured and parametric fluorescence measured nonlinear coefficients for lithium iodate also needs to be resolved.

It is possible to make accurate measurements of nonlinear optical coefficients using the technique of second-harmonic generation provided a great deal of care is used in making the measurements and high optical quality fundamental radiation is used. The development of automatic data acquisition and reduction techniques and the availability of well-characterized highly coherent lasers will make further accurate measurements tractable. The wide range of nonlinear coefficient values that have been obtained over the past 25 years underscores the need to use well-characterized high-quality sources of fundamental radiation in nonlinear optical frequency conversion.

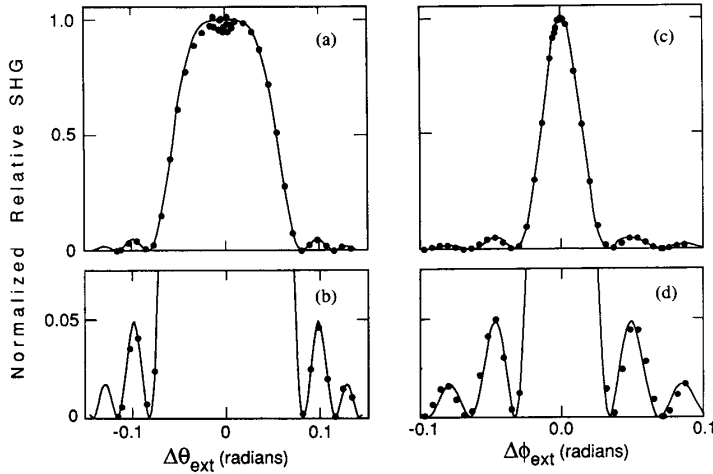


Fig. 8. Phase-matching tuning curves of an antireflection-coated KTP crystal for noncritical rotation [(a) and (b)] and critical rotation [(c) and (d)]. Data points show the observed tuning curves, and solid lines show the calculated tuning curves.

TABLE III
NONLINEAR OPTICAL COEFFICIENTS

Crystal	Nonlinear Optical Coefficient ^a (10^{-12} m/V)	Miller's Delta ($10^{-2} \text{ m}^2/\text{C}$)
KDP	$d_{36} = 0.38$	$\delta_{36} = 2.4$
KD*P	$d_{36} = 0.37$	$\delta_{36} = 2.4$
LiIO ₃	$d_{31} = -4.1$	$\delta_{31} = -3.8$
5% MgO:LiNbO ₃	$d_{31} = -4.7$	$\delta_{31} = -0.84$
BaB ₂ O ₄	$d_{\text{eff}} = 1.94$	
	$ d_{22} = 2.2^b$	$ \delta_{22} = 4.5$
KTP	$d_{\text{eff}} = 3.18$	
	$ d_{15} = 2.6^c$	$ \delta_{15} = 2.9$
	$ d_{24} = 3.3$	$ \delta_{24} = 2.5$

^aNonlinear coefficients are given for 1064 to 532 nm second harmonic generation.

^bAssumes that $|d_{31}| \ll |d_{22}|$ for BaB₂O₄ [24].

^cUsing $|d_{24}|/|d_{15}| = 1.25$ [33] and assuming d_{24} and d_{15} have the same sign.

APPENDIX

Some detailed aspects of nonlinear frequency conversion in birefringent crystals are considered in this Appendix. An anisotropic-media Green's function analysis is used to show that the treatment used here is appropriate for quantitative analysis of second-harmonic generation under near-field conditions. Only under tight focusing conditions will birefringence cause some astigmatism and aberration that is not already included in the analysis.

A central assumption of the Boyd and Kleinman treatment of harmonic generation by focused beams [11] is that a Gaussian harmonic beam is generated in each infinitesimal slab increment of a nonlinear crystal through which a Gaussian fundamental beam is propagated. In the case of type I phase matching in a negative uniaxial crystal, the fundamental beam is an ordinary wave and the harmonic is extraordinary. It is further assumed that the extraordinary harmonic beam has the same focal position f and the same confocal parameter b as the fundamental

beam. However, the transverse position of the extraordinary beam is displaced in a way that causes it to propagate with the appropriate birefringent walkoff. This result was derived by Kleinman *et al.* [34] using an isotropic-media Green's function modified to include birefringent walkoff.

We proceed with the anisotropic-media analysis, expressing results in a form similar to [34] to facilitate comparison. Assume that the nonlinear crystal exists between $z = 0$ and $z = l$, and is imbedded in a medium with identical linear birefringent properties, but with no nonlinearity. The harmonic electric field at a point r is given by

$$E_2(r, t) = \frac{\exp(-2i\omega t)}{4\pi\epsilon_0} \int_V \exp\{-\alpha_2(z - z')/2\} \cdot \gamma G(r, r') \cdot \mathcal{P}^{NL}(r') dr'. \quad (A1)$$

Here, 2ω is the angular frequency of the harmonic, and α_2 is the absorption coefficient at the harmonic frequency. The dyadic projection operator is defined by

$$\gamma = \frac{4\pi i\omega}{cn_e(\theta)} \hat{u}\hat{u} \quad (A2)$$

where $n_e(\theta)$ is the index of refraction for the extraordinary harmonic wave, and \hat{u} is a unit vector in the direction of the electric field of the harmonic wave. The nonlinear polarization produced by an ordinary Gaussian fundamental beam propagating in the z direction is

$$\mathcal{P}^{NL}(r') = \mathcal{P}_0 \frac{\exp\{2ik_1 z' - \alpha_1 z'\}}{(1 + ir')^2} \cdot \exp\left\{-\frac{2(x'^2 + y'^2)}{w_0^2(1 + ir')}\right\} B(z') \quad (A3)$$

where $\tau' = 2(z' - f)/b$ and $B(z') = 1$ for $0 \leq z' \leq 1$ and 0 elsewhere. The fundamental wavevector is k_1 , and α_1 is the absorption coefficient of the fundamental. Everything to this point is identical to [34] except for the anisotropic Green's function.

The Green's function for an anisotropic dielectric is [10]

$$\gamma G(\mathbf{r}, \mathbf{r}') = \hat{\mathbf{u}}\hat{\mathbf{u}} \left(\frac{\omega}{c} \right)^2 \frac{1}{k_e \sqrt{K_e} \cos \rho} \frac{\exp \{ ik_e \cdot (\mathbf{r} - \mathbf{r}') \}}{|\mathbf{r} - \mathbf{r}'|}. \quad (\text{A4})$$

Equation (A4) differs from the Green's function used in [34] by the factor $k_e \sqrt{K_e} \cos \rho$ in the denominator where K_e is the Gaussian curvature of the surface defined by $k_e(2\omega)$ and ρ is the birefringent walkoff angle. For an isotropic medium, $k_e \sqrt{K_e} \cos \rho$ is one, and the Green's functions become the same. As an example of an anisotropic material, consider LiIO₃ oriented for phase-matched, type I, 1064 \rightarrow 532 nm second-harmonic generation for which $k_e \sqrt{K_e} \cos \rho \approx 1.10$.

However, the factor becomes $1/\cos \rho \approx 1$ when the variation of k_e with direction is included in the x' and y' integration of (A1). The paraxial expansion used to perform the integration is

$$\begin{aligned} & \frac{\exp \{ ik_e \cdot (\mathbf{r} - \mathbf{r}') \}}{|\mathbf{r} - \mathbf{r}'|} \\ &= \frac{\exp \{ 2ik_1(z - z') \}}{(z - z')} \\ & \cdot \exp \left\{ \frac{-ik_1[x - x' - \rho(z - z')]}{2k_1 \kappa_x(z - z')} \right\} \\ & - \frac{ik_1(y - y')^2}{2k_1 \kappa_y(z - z')}. \end{aligned} \quad (\text{A5})$$

Phase matching is assumed in this expression, and κ_x and κ_y are the principal curvatures of the surface defined by k_e (note $K_e = \kappa_x \kappa_y$). Again, for isotropic material, we would have $2k_1 \kappa_x = k_e \kappa_x = 1$ and $2k_1 \kappa_y = k_e \kappa_y = 1$, and (A5) would become identical to the expansion used in [34].

Completing the x' and y' integrations of (A1) using (A4) and (A5), we have

$$\begin{aligned} E_2(\mathbf{r}) = \gamma \cdot \mathcal{G}_0 \frac{\exp \{ 2ik_1 z - \alpha_2 z/2 \}}{\cos \rho} \\ \cdot \int_0^l \exp \left\{ \frac{-2[x - \rho(z - z')]}{w_0^2(1 + i\tau_x)} \right\} \\ - \frac{2y^2}{w_0^2(1 + i\tau_y)} \left\{ \frac{e^{-\alpha_2 z'} dz'}{(1 + i\tau')^2} \right\} \end{aligned} \quad (\text{A6})$$

where

$$\tau_x = 2 \{ z - [f/k_e \kappa_x - (1/k_e \kappa_x - 1)z'] \} k_e \kappa_x / b \quad (\text{A7})$$

and

$$\tau_y = 2 \{ z - [f/k_e \kappa_y - (1/k_e \kappa_y - 1)z'] \} k_e \kappa_y / b. \quad (\text{A8})$$

We could further manipulate the expressions (A7) and (A8) to have x -distribution and y -distribution focal positions and confocal parameters, but it is unnecessary for our purposes. We can project the solution back to the plane $z = l$, and take that as the exit surface of the crystal. With the experimental conditions of these measurements, we are in the near field with $\tau \ll 1$ at this plane. In using (8), we had assumed that τ could be ignored, and the small changes in τ given by the last two equations are of no significance. In the approximation that $\tau_x \approx \tau_y \approx \tau = (z - f)/b$, (A6) becomes the same as [34, eq. (4.19)], the result mentioned above which leads to (2.9) of the Boyd and Kleinman focused beam analysis [11].

For parametric fluorescence in negative uniaxial crystals such as LiIO₃ or LiNbO₃, the scattered radiation or parametrically generated noise is ordinary, and an isotropic analysis of the scattering is adequate. The pump radiation used for these parametric fluorescence measurements, however, is extraordinary. Therefore, it is necessary to use the angle of propagation plus the walkoff angle ($\theta + \rho$) when calculating components of the extraordinary electric field of the pump radiation that lie in the direction of the principal axes of the crystal. In both parametric fluorescence measurements and second-harmonic measurements in these crystals, the measured effective nonlinear coefficients must be converted to components of the nonlinear optical tensor using the angle ($\theta + \rho$) [11]. For LiNbO₃ with $\theta = 90^\circ$, $\rho = 0$, and there is no change from using θ instead of ($\theta + \rho$). For LiIO₃ with $\theta = 30.2^\circ$, $\rho = 4.26^\circ$, the effective nonlinear coefficient is increased by 1.12 for a given value of d_{31} using ($\theta + \rho$) instead of θ . This factor is not adequate to account for the discrepancy between d_{eff} measured here by SHG and previous measurements by parametric fluorescence.

ACKNOWLEDGMENT

The authors express their appreciation to the organizations and individuals who provided materials for this investigation. The barium metaborate crystals were supplied by R. Route and R. Feigelson of Stanford University and C.-T. Chen of the Fujian Institute. S. Velsko of Lawrence Livermore National Laboratories loaned the potassium dihydrogen phosphate crystal. The magnesium oxide-doped lithium niobate material was supplied by Crystal Technology, Inc., Palo Alto, CA. The authors also express their thanks to M. K. Reed, who designed the spatial filter and gave valuable advice on the operation of the injection-seeded laser.

REFERENCES

[1] Y. X. Fan, R. C. Eckardt, R. L. Byer, J. Nolting, and R. Wallenstein, "Visible BaB₂O₄ optical parametric oscillator pumped at 355 nm by a single-axial-mode pump source," *Appl. Phys. Lett.*, vol. 53, pp. 2014-2016, 1988.

[2] R. S. Craxton, "High efficiency frequency tripling schemes for high-power Nd:glass lasers," *IEEE J. Quantum Electron.*, vol. QE-17, pp. 1771-1782, 1982.

[3] D. Eimerl, "Electro-optic, linear, and nonlinear optical properties of KDP and its isomorphs," *Ferroelect.*, vol. 72, pp. 95-139, 1987.

[4] G. E. Francois, "cw measurement of the optical nonlinearity of ammonium dihydrogen phosphate," *Phys. Rev.*, vol. 143, pp. 597-600, 1966.

[5] J. E. Bjorkholm and A. E. Siegman, "Accurate cw measurement of optical second-harmonic generation in ammonium dihydrogen phosphate and calcite," *Phys. Rev.*, vol. 154, pp. 851-860, 1967.

[6] S. Singh, "Nonlinear optical materials," in *Handbook of Laser Science and Technology*, vol. III, M. J. Weber, Ed. Boca Raton, FL: CRC Press, 1986, pp. 3-228.

[7] M. M. Choy and R. L. Byer, "Accurate second-order susceptibility measurements of visible and infrared nonlinear materials," *Phys. Rev. B*, vol. 14, pp. 1693-1706, 1976.

[8] A. J. Campillo and C. L. Tang, "Spontaneous parametric scattering of light in LiIO₃," *Appl. Phys. Lett.*, vol. 16, pp. 242-244, 1970.

[9] S. K. Kurtz, J. Jephagnon, and M. M. Choy, "Nonlinear dielectric susceptibilities," in *Landolt-Bornstein, Numerical Data and Fundamental Relationships in Science and Technology, New Series, Group III, Crystals and Solid State Physics, Vol. 11*, K.-H. Hellwege and A. M. Hellwege, Eds. Berlin: Springer, 1979, pp. 671-743.

[10] M. Lax and D. F. Nelson, "Light scattering in crystals with surface corrections," in *The Theory of Light Scattering in Condensed Matter*, V. N. Agranovich and J. L. Birman, Eds. New York: Plenum, 1976, pp. 371-390.

[11] G. D. Boyd and D. A. Kleinman, "Parametric interactions of focused Gaussian light beams," *J. Appl. Phys.*, vol. 39, pp. 3597-3639, 1968.

[12] J. A. Armstrong, N. Bloembergen, J. Ducuing, and P. S. Pershan, "Interaction between light waves in a nonlinear dielectric," *Phys. Rev.*, vol. 127, pp. 1918-1939, 1962.

[13] S. K. Kurtz, "Measurement of nonlinear optical susceptibilities," in *Quantum Electronics: A Treatise, Vol. 1, Part A*, H. Rabin and C. L. Tang, Ed. New York: Academic, 1975, pp. 209-281.

[14] R. L. Byer, "Parametric oscillators and nonlinear materials," in *Nonlinear Optics*, P. G. Harper and B. S. Wherrett, Eds. San Francisco, CA: Academic, 1977, pp. 47-160.

[15] R. C. Miller, "Optical second harmonic generation in piezoelectric crystals," *Appl. Phys. Lett.*, vol. 5, pp. 17-19, 1964.

[16] J. E. Midwinter and J. Warner, "The effects of phase matching method and of uniaxial crystal symmetry on the polar distribution of second-order nonlinear optical polarization," *Brit. J. Appl. Phys.*, vol. 16, pp. 1135-1142, 1965.

[17] F. Zernike, Jr., "Refractive indices of ammonium dihydrogen phosphate and potassium dihydrogen phosphate between 2000 Å and 1.5 μ," *J. Opt. Soc. Amer.*, vol. 54, pp. 1215-1220, 1964; *J. Opt. Soc. Amer.*, vol. 55, pp. 210-211, 1965.

[18] K. W. Kirby, C. S. Hoeffer, and L. G. Deshazer, unpublished. The Sellmeier dispersion equations obtained by these authors are reproduced in [3].

[19] K. Kato, "Second-harmonic generation to 2048 Å in β-BaB₂O₄," *IEEE J. Quantum Electron.*, vol. QE-22, pp. 1013-1014, 1986.

[20] R. Herbst, unpublished. This Sellmeier equation for LiIO₃ is reproduced in [9].

[21] G. J. Edwards and M. Lawrence, "A temperature-dependent dispersion equation for congruently grown lithium niobate," *Opt. Quantum Electron.*, vol. 16, pp. 373-375, 1984. These dispersion equations for congruent LiNbO₃ were modified by changing the extraordinary coefficient A_1 from 4.5820 to 4.55207 to obtain agreement with phase-matching temperatures observed for 5%MgO:LiNbO₃ in harmonic and parametric generation measurements.

[22] T. Y. Fan, C. E. Huang, B. Q. Hu, R. C. Eckardt, Y. X. Fan, R. L. Byer, and R. S. Feigelson, "Second harmonic generation and accurate index of refraction measurements in flux-grown KTiPO₄," *Appl. Opt.*, vol. 26, pp. 2390-2394, 1987.

[23] C.-T. Chen, Y. X. Fan, R. C. Eckardt, and R. L. Byer, "Recent developments in barium borate," *Proc. SPIE*, vol. 681, pp. 12-19, 1986.

[24] D. Eimerl, L. Davis, and S. Velsko, "Optical, mechanical, and thermal properties of barium borate," *J. Appl. Phys.*, vol. 62, pp. 1968-1983, 1987.

[25] R. L. Byer and S. E. Harris, "Power and bandwidth of spontaneous parametric emission," *Phys. Rev.*, vol. 168, pp. 1064-1068, 1968.

[26] J. L. Nightingale, W. J. Silva, G. E. Reade, A. Rybicki, W. J. Kozlovsky, and R. L. Byer, "Fifty percent conversion efficiency second harmonic generation in magnesium oxide doped lithium niobate," *Proc. SPIE*, vol. 681, pp. 20-24, 1986.

[27] D. A. Bryan, R. R. Rice, R. Gerson, H. E. Tomaschke, K. L. Sweeney, and L. E. Halliburton, "Magnesium-doped lithium niobate for higher optical power applications," *Opt. Eng.*, vol. 24, pp. 138-143, 1985.

[28] W. J. Kozlovsky, C. D. Nabors, and R. L. Byer, "Efficient second harmonic generation of a diode-laser-pumped CW Nd:YAG laser using monolithic MgO:LiNbO₃ external resonant cavities," *IEEE J. Quantum Electron.*, vol. 24, pp. 913-919, 1988.

[29] E. O. Ammann and S. Guch, Jr., "1.06-0.53 μm second harmonic generation using congruent lithium niobate," *Appl. Phys. Lett.*, vol. 52, pp. 1374-1376, 1988.

[30] R. C. Miller, D. A. Kleinman, and A. Savage, "Quantitative studies of optical harmonic generation in CdS, BaTiO₃, and KH₂PO₄ type crystals," *Phys. Rev. Lett.*, vol. 11, pp. 146-149, 1963.

[31] J. P. van der Ziel and N. Bloembergen, "Temperature dependence of optical harmonic generation in KH₂PO₄ ferroelectrics," *Phys. Rev. A*, vol. 135, pp. 1662-1669, 1964.

[32] V. S. Suvorov, A. S. Sonin, and I. S. Rez, "Some nonlinear optical properties of crystals in the KDP group," *Sov. Phys.-JETP*, vol. 26, pp. 33-37, 1968.

[33] F. C. Zumsteg, J. D. Bierlein, and T. E. Grier, "K_xRb_{1-x}TiOPO₄: A new nonlinear optical material," *J. Appl. Phys.*, vol. 47, pp. 4980-4985, 1976.

[34] D. A. Kleinman, A. Ashkin, and G. D. Boyd, "Second-harmonic generation of light by focused laser beams," *Phys. Rev.*, vol. 145, pp. 338-379, 1966.



Robert C. Eckardt (M'84), was born in Chicago, IL in 1940. He received the B.S. degree in engineering physics from the University of Illinois, Urbana, in 1963 and the M.S. degree in physics from the University of Maryland, College Park, in 1970.

From 1963 to 1983 he was a physicist and Research Physicist at the Naval Research Laboratory, Washington, DC. In 1983 he joined Stanford University, Stanford, CA, as a Senior Research Associate in the Ginzton Laboratory of Physics. His research interests include nonlinear optics and laser development.

Mr. Eckardt is a member of the Optical Society of America and Sigma Xi.



Hisashi Masuda was born in Tokyo, Japan in 1960. He received the B.E. degree in applied physics from the University of Tokyo, Japan, in 1984, and the M.S. degree in applied physics from Stanford University, Stanford, CA, in 1988.

Since 1984 he has been with the Sony Corporation, Tokyo, Japan, developing optical heads of optical disk systems. He also worked at Stanford University as a visiting scientist for the research on nonlinear optics in 1989. His current research interest includes new types of optical heads, frequency conversion of coherent light sources and stabilization of laser cavities.

Yuan Xuan Fan, photograph and biography not available at the time of publication.

Robert L. Byer (M'75-SM'83-F'87), for a photograph and biography, see p. 157 of the January 1990 issue of this JOURNAL.